

# TURBULENT RAYLEIGH-BENARD CONVECTION UNDER TIME-MODULATED ROTATION CONDITIONS

**Bernard J. Geurts**

Multiscale Modeling and Simulation, Faculty EEMCS  
University of Twente  
P.O. Box 217, 7500 AE Enschede, The Netherlands  
B.J.Geurts@utwente.nl

**Rudie Kunnen**

Fluid Dynamics Laboratory, Faculty of Applied Physics  
Eindhoven University of Technology  
P.O. Box 513, 5600 MB Eindhoven, The Netherlands  
r.p.j.kunnen@tue.nl

## ABSTRACT

We present results of direct numerical simulation of turbulent flow in a rotating cylindrical Rayleigh-Bénard system of unit aspect ratio in which the rotation frequency is modulated in time. Associated with the time-dependent rotation rate the Euler force arises in addition to the Coriolis and centrifugal forces in the governing equations. This Euler force acts in the circumferential direction and has a marked effect on the turbulent flow structures and the associated heat transfer efficiency. We observe a regime with strong Euler forces in case the modulation of the rotation rate is sufficiently rapid. Sheared velocity structures dominate the vertical boundary layers near the cylinder walls, while a strong thermal column of a characteristic size arises in the core of the system, along the axis of rotation. The Nusselt number is observed to become rapidly oscillating at frequencies associated with the modulation frequency. Compared to the case of constant rotation rate the Nusselt number is increased considerably. The heat transfer displays a striking dynamics; after relatively long periods of strongly increasing Nusselt number, events of sudden collapse of the thermal structure in the core of the system occur. A detailed illustration of such a collapse in the Nusselt number shows the almost complete disappearance of the thermal column and associated reduction of the capacity to transfer heat in the system.

## INTRODUCTION

Many flows in nature and technology are simultaneously driven by buoyant convection as well as influenced by rotation. Typical examples are found in the large-scale geophysical flows in the atmosphere and the oceans on our Earth. Understanding these is essential for predicting heat and mass transfer, and hence essential for weather and climate predictions. Also in many technological applications buoyancy and rotation are key mechanisms, e.g., in cooling or controlled crystal growth. A simple model that captures the dynamic consequences arising from interactions between these central mechanisms is found in rotating

Rayleigh-Bénard convection: a fluid layer enclosed vertically between parallel rotating walls is heated from below and cooled from above. The dynamics of rotating Rayleigh-Bénard (RRB) convection, in case of constant rotation rate, is governed by three dimensionless parameters, i.e., the Prandtl number  $\sigma$ , the Rayleigh number  $Ra$  and the Rossby number  $Ro$  Kunnen (2008). In this paper we investigate the dynamics in case the rotation rate  $\Omega$  becomes a function of time. This time-dependence introduces additional ‘Rossby’ numbers that quantify the depth and the frequency of the modulation of the rotation rate. The time-dependent rotation gives rise to a so-called Euler force in the governing equations, which may have a strong influence on the flow structures in the turbulent flow and associated consequences for the effectiveness of the heat transfer. We present direct numerical simulation (DNS) results for a range of time-modulated rotation rates and focus on thermal transport.

We focus on the question to what extent time-modulated rotation affects the heat transport properties of a cylindrical Rayleigh-Bénard system. Extensive numerical and experimental studies were conducted in recent years on this system in case of a constant rotation rate Kunnen *et al.* (2008); Stevens *et al.* (2010). It was shown that the Nusselt number increases by several tens of percents relative to the non-rotating case, provided the Rossby and Prandtl numbers are taken in the proper range. The increased Nusselt number could be explained by the presence of vortical plumes that enable the extra vertical transport process known as Ekman pumping Rossby (1969); Julien *et al.* (1996); Kunnen *et al.* (2010). Conversely, in experimental investigations at constant rotation rate using cryogenic helium (Prandtl number  $\sigma = 0.7$ ), no heat transfer increase was observed Niemela *et al.* (2010). These authors found that when the rotation rate varied periodically in time, a sharp transition to a state of significantly enhanced heat transport could be observed at appropriate modulation rates. In addition to the enhanced heat transfer, the interest in modulated rotation stems from the more general research in ‘resonant turbulence’ Kuczaj *et al.* (2006) where external agitation of a flow is considered to qualitatively alter the

flow and intensify the dominant processes that take place. As such, it is part of the field of ‘physical control’ of fluid systems, which is crucial in a variety of technological applications.

The inclusion of a time-dependent rotation rate expressed by the so-called Euler force may qualitatively alter the flow from a condition of a domain filling large-scale circulation (LSC; occurring at low constant rotation rates) or dispersed local thermal plumes (at high constant rotation rates), to a more or less segregated situation in which a pronounced thermal column forms along the centerline of the domain and highly sheared structures appear in the boundary layer near the vertical sidewalls. A dominant Euler force yields very complex flow dynamics in which a long-time build-up of thermal structures arises in an oscillating manner, interspersed by events of very abrupt and considerable collapse with associated strong reduction of the thermal transport efficiency, as quantified by the Nusselt number  $Nu$ . This presents an interesting challenge in physical control of such turbulent flow, aimed at building up high- $Nu$  flow structures by modulated rotation, but avoiding the  $Nu$ -collapse.

The organization of this paper is as follows. We first present the governing equations and discuss the numerical method. Subsequently, the effect of time-modulated rotation is shown in terms of the changes in the turbulent flow structures that arise. The consequences for the transport of heat are discussed afterwards and the paper is completed with concluding remarks.

## GOVERNING EQUATIONS AND NUMERICAL METHOD

We consider cylindrical domains filled with water, of height  $H$  and diameter  $D = H$ , i.e., we study domains with aspect ratio  $\Gamma = D/H = 1$ . The domain is allowed to rotate about the vertical ( $z$ ) axis with rotation rate  $\mathbf{\Omega}(t) = \Omega(t)\hat{\mathbf{z}}$  where  $\hat{\mathbf{z}}$  denotes the unit vector in the  $z$  direction. We consider the flow in a co-rotating coordinate frame  $(\hat{\mathbf{x}}, \hat{\mathbf{y}}, \hat{\mathbf{z}})$  rotating with  $\mathbf{\Omega}(t)$  relative to inertial frame  $(\hat{\mathbf{X}}, \hat{\mathbf{Y}}, \hat{\mathbf{Z}})$ . The transformation of the velocity between the co-rotating and the inertial frame is given by

$$\left(\frac{d\mathbf{r}}{dt}\right)_I = \left(\frac{d\mathbf{r}}{dt}\right)_R + (\mathbf{\Omega}(t) \times \mathbf{r}) \quad (1)$$

where the position vector  $\mathbf{r} = r_x\hat{\mathbf{x}} + r_y\hat{\mathbf{y}} + r_z\hat{\mathbf{z}}$  and the subscript  $I$  ( $R$ ) refers to the inertial (rotating) frame of reference. For the acceleration we find likewise

$$\begin{aligned} \left(\frac{d^2\mathbf{r}}{dt^2}\right)_I &= \left(\frac{d^2\mathbf{r}}{dt^2}\right)_R + \underbrace{2\mathbf{\Omega}(t) \times \left(\frac{d\mathbf{r}}{dt}\right)_R}_{\text{Coriolis}} + \underbrace{\mathbf{\Omega}(t) \times \mathbf{\Omega}(t) \times \mathbf{r}}_{\text{Centrifugal}} \\ &+ \underbrace{\frac{d\mathbf{\Omega}(t)}{dt} \times \mathbf{r}}_{\text{Euler}} \end{aligned} \quad (2)$$

in which we have identified the Coriolis, centrifugal and Euler forces.

The time-modulation of the rotation rate is taken as

$$\mathbf{\Omega}(t) = \mathbf{\Omega}_0 + \Delta\mathbf{\Omega} \sin(\omega t) \quad (3)$$

where we denote the mean rotation rate by  $\mathbf{\Omega}_0$ , the depth of modulation by  $\Delta\mathbf{\Omega}$  and the frequency of modulation by  $\omega$ . This can equivalently be expressed in terms of three ‘Rossby numbers’. In face, multiplying by  $2H/U$  we find

$$\frac{1}{Ro}(t) = \frac{1}{Ro_0} + \frac{1}{Ro^*} \sin\left(\frac{t}{2Ro_\omega}\right) \quad (4)$$

where

$$Ro_0 = \frac{U}{2H\Omega_0} ; Ro^* = \frac{U}{2H\Delta\Omega} ; Ro_\omega = \frac{U}{2H\omega} \quad (5)$$

These parameters can be varied independently, giving detailed control over the precise flow regime that dominates the turbulent transport.

The governing equations that describe incompressible flow in a co-rotating frame of reference can be written as  $\nabla \cdot \mathbf{u} = 0$  for the conservation of mass,

$$\begin{aligned} \partial_t \mathbf{u} + (\mathbf{u} \cdot \nabla) \mathbf{u} &= -\nabla p + g\alpha T \hat{\mathbf{z}} + \nu \nabla^2 \mathbf{u} - 2\mathbf{\Omega}(t) \hat{\mathbf{z}} \times \mathbf{u} \\ &- r \frac{d\mathbf{\Omega}(t)}{dt} \hat{\boldsymbol{\theta}} \end{aligned} \quad (6)$$

for conservation of momentum, using the Boussinesq approximation and

$$\partial_t T + (\mathbf{u} \cdot \nabla) T = \kappa \nabla^2 T \quad (7)$$

for the transport of heat. In this formulation, we absorbed the centrifugal contribution into  $\nabla p$  where  $p$  denotes the total dynamic pressure. Moreover,  $\mathbf{u}$  denotes the velocity field,  $g$  the gravitational acceleration,  $\alpha$  the thermal expansion coefficient,  $T$  the temperature,  $\nu$  the kinematic viscosity and  $\kappa$  the thermal diffusivity. In non-dimensional form — using the convective velocity scale  $U = \sqrt{g\alpha\Delta TH}$ , temperature scale  $\Delta T$  and length scale  $H$  — the momentum equation may be expressed as

$$\begin{aligned} \partial_t \mathbf{u} + (\mathbf{u} \cdot \nabla) \mathbf{u} &= -\nabla p + T \hat{\mathbf{z}} + \sqrt{\frac{\sigma}{Ra}} \nabla^2 \mathbf{u} \\ &- \left[ \frac{1}{Ro_0} + \frac{1}{Ro^*} \sin\left(\frac{t}{2Ro_\omega}\right) \right] \hat{\mathbf{z}} \times \mathbf{u} \\ &- \frac{1}{4Ro^*Ro_\omega} \cos\left(\frac{t}{2Ro_\omega}\right) r \hat{\boldsymbol{\theta}} \end{aligned} \quad (8)$$

We observe a directly modulated Coriolis term (second line) and the Euler term (third line) which acts in the circumferential direction only. The non-dimensional heat equation can be written as

$$\partial_t T + (\mathbf{u} \cdot \nabla) T = \frac{1}{\sqrt{\sigma Ra}} \nabla^2 T \quad (9)$$

where well-known dimensionless groups appear:  $Ra = (g\alpha\Delta TH^3)/(\nu\kappa)$  the Rayleigh number in terms of the temperature difference  $\Delta T$  between bottom and top wall,  $\sigma = \nu/\kappa$  the Prandtl number, and  $Ro_0, Ro^*, Ro_\omega$  the Rossby numbers. The boundary conditions are taken as  $\mathbf{u} = \mathbf{0}$ ,

$T = 1$  at the bottom plate,  $\mathbf{u} = \mathbf{0}$ ,  $T = 0$  at the top plate and  $\mathbf{u} = \mathbf{0}$ ,  $\partial_r T = 0$  at the sidewall.

The direct numerical simulations were based on an extension of the method by Verzicco & Orlandi (1996). We consider as working fluid pure water with  $\sigma = 6.4$  and investigate turbulent flow at  $Ra = 10^9$ , identical to the value used in the study of Kunnen *et al.* (2006), in order to facilitate comparison with the constant rotation case. The spatial resolution is taken as  $(n_r, n_\theta, n_z) = (385, 193, 385)$ , which was found adequate to also resolve the finer scales of the flow. We work in cylindrical coordinates in which case several terms in the governing equations possess a factor  $1/r$  with  $r$  the radial coordinate. These terms need special treatment near the cylinder axis. We solve therefore equations for the state vector  $(ru_r, u_\phi, u_z)$  on a staggered grid which avoids the centerline. The equations are discretized by a central finite-difference formulation of second order accuracy. Further applications can be found in Geurts (2001).

## TURBULENT FLOW STRUCTURES

In this section we present the turbulent flow structures arising at constant and at time-modulated rotation.

### Constant rotation rate

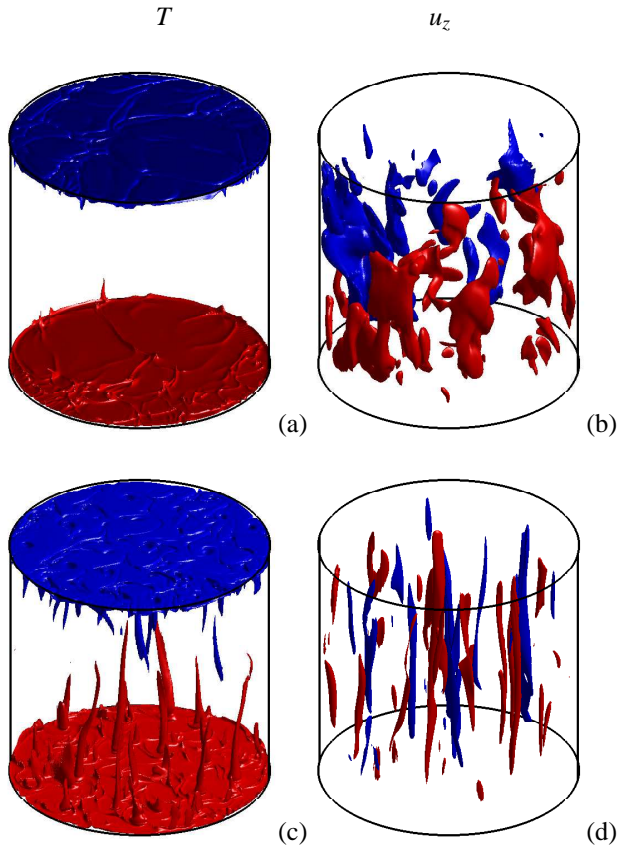


Figure 1. Snapshots of temperature (a, c) and vertical velocity (b, d) isosurfaces at constant rotation rate with  $Ro_0 = 5$  (a, b) and  $Ro_0 = 0.1$  (c, d).

Simulations at various rotation rates show that the organization of the flow into coherent structures is strongly

dependent on rotation. For small rotation rates the domain-filling large-scale circulation (LSC), well-known from non-rotating convection, is the dominant feature. At larger rotation rates an irregular, unsteady array of vortical plumes is found. The turbulence intensity is reduced by rotation, and the vertical homogeneity increases. At even higher rotation rates a striking dynamic columnar patterns of vortices emerges Kunnen *et al.* (2008). Vortical structuring in a Rayleigh-Bénard system at  $Ro_0 = 0.1$  and 5 is provided in Fig. 1. The slow rotation ( $Ro_0 = 5$ ) shows a clear large scale circulation with a clear region of upwelling (blue) next to a single region of downwelling (red). The faster rotation ( $Ro_0 = 0.1$ ) displays a much more detailed structure with highly elongated velocity structures, spread quite evenly over the domain. Correspondingly, the temperature shows strongly localized thermal plumes at fast rotation rates and a much more even temperature boundary layer at slow rotation.

### Time-modulated rotation rate

The effect of time-modulation of the rotation rate depends strongly on the modulation frequency  $Ro_\omega$ . Taking fast ( $Ro_0 = 0.1$ ) and slow ( $Ro_0 = 5$ ) rotation as points of reference by choosing  $Ro_0 = 2.45$  and  $Ro^* = 2.55$ , we may traverse from slow to fast rather slowly ( $Ro_\omega > 1$ ) or rather quickly ( $Ro_\omega < 1/10$ ). The modulation frequency is seen to have only a modest structural effect at  $Ro_\omega = 0.5$  as can be inferred from Fig. 2(a, b). The flow is mainly in a state reminiscent of the LSC state at constant rotation. Increasing the modulation frequency, i.e., increasing the relevance of the Euler force on the flow, is seen to yield a strong thermal structure centered around the axis of the cylinder, while clear sheared turbulence structures near the vertical sidewalls are seen in the vertical velocity isosurfaces. A closer look at these sheared boundary layer structures is provided in Figure 3 in which we show a top-view of isosurfaces of the vertical velocity. With increasing modulation frequency, i.e., at reduced  $Ro_\omega$ , finer structure appear near the vertical walls. These structures seem not to penetrate into a ‘middle section’ of the flow domain that is occupied by the ‘thermal column’, which thereby also attains a characteristic width.

## DYNAMICS OF HEAT TRANSFER

In order to quantify the consequences of time-modulated rotation on the efficiency with which heat can be transferred from the hot bottom plate to the colder top plate, we concentrate on the Nusselt number  $Nu$ . A convenient expression with which the time-dependent  $Nu$  can be obtained is

$$Nu(t) = \langle \partial_z T \rangle \quad (10)$$

where  $\langle \cdot \rangle$  denotes averaging over the top and/or bottom wall. We first consider  $Nu$  for the case of constant rotation and turn to time-modulation effects subsequently.

### Constant rotation rate

In Figure 4(a) we show the dependence of the Nusselt number on time  $t$  for several constant rotation rates. We observe that after a short transient up to  $t \approx 50$  the Nusselt number becomes an oscillating function of time, characterized by a range of frequencies. No clear, distinctive

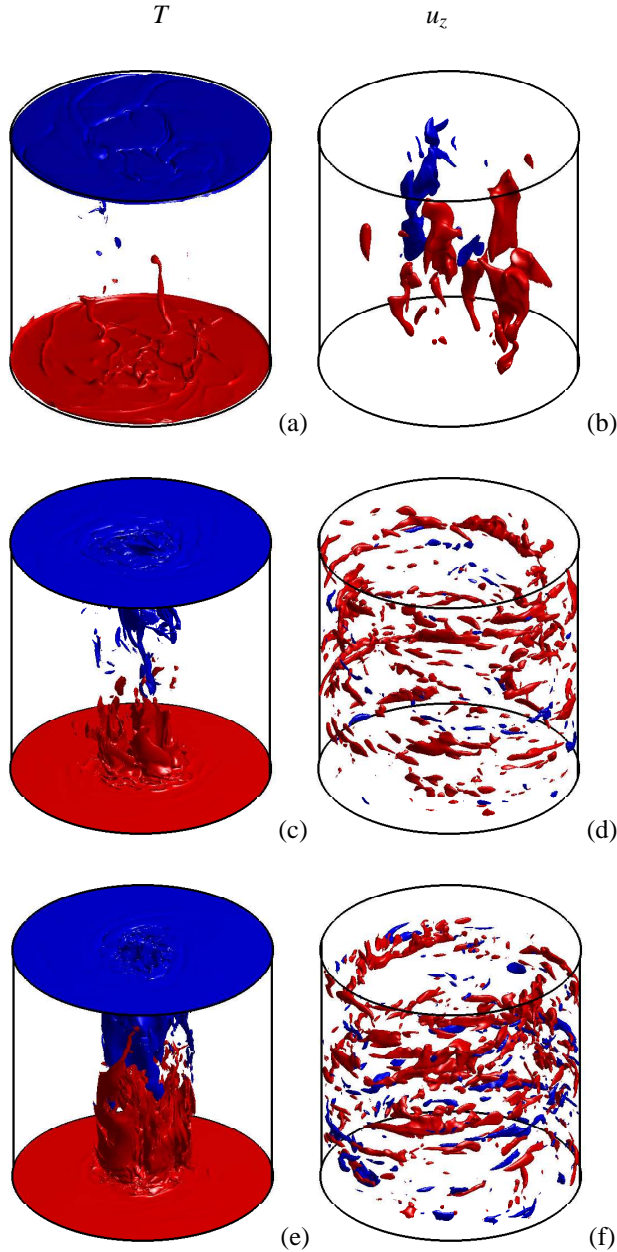


Figure 2. Snapshots of temperature (a, c, e) and vertical velocity (b, d, f) isosurfaces at  $Ro_0 = 2.45$ ,  $Ro^* = 2.55$  and  $Ro_\omega = 0.5$  (a, b),  $Ro_\omega = 0.2$  (c, d) and  $Ro_\omega = 0.1$  (e, f).

pattern is seen in these time histories, other than the occurrence of somewhat higher frequency components in the response as the rotation rate increases. When averaged also over time  $t$ , employing intervals up to  $t = 500$  to reach statistical convergence of the averages, we observe that the relative Nusselt number, i.e.,  $Nu(Ro_0)$  normalized with the value in the non-rotating situation, has a definite maximum of about 1.2 for  $Ro_0 \approx 0.2$ . This phenomenon was also observed earlier in literature, and the simulation results compare quite well with other sources as may be inferred in Figure 4(b). We also notice that at the slow ( $Ro_0 = 5$ ) and the fast ( $Ro_0 = 0.1$ ) rotation rates presented in Figure 1 the time-averaged relative Nusselt number is virtually the same and close to unity, albeit with strongly different turbulent flow structures.

In the sequel we consider in more detail the Nusselt response when traversing the interval  $0.1 \leq Ro(t) \leq 5$  with

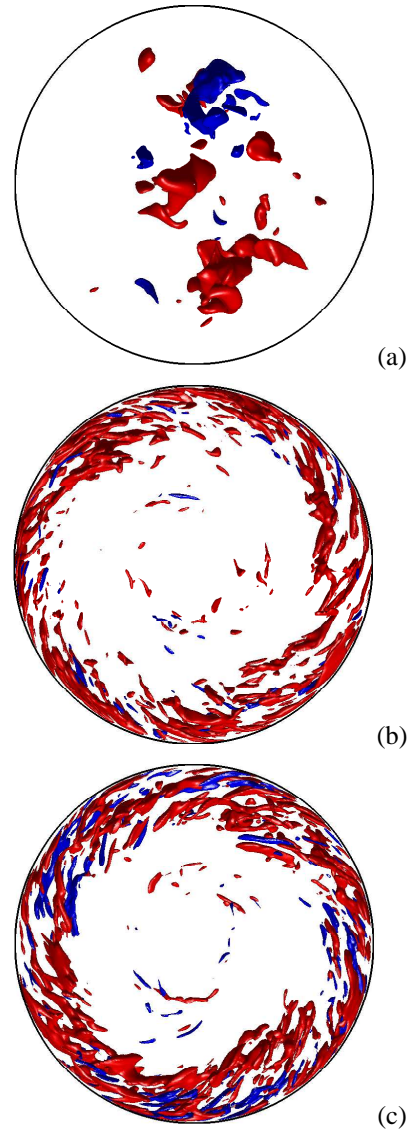


Figure 3. Snapshots of top-view of the vertical velocity at  $Ro_0 = 2.45$ ,  $Ro^* = 2.55$  and  $Ro_\omega = 0.5$  (a),  $Ro_\omega = 0.2$  (b) and  $Ro_\omega = 0.1$  (c).

different frequencies.

### Time-modulated rotation rate

In Figure 5 we present the response of the Nusselt number in case of time-modulated rotation rate. Compared to the constant rotation rate we notice a clear increase in the variability with which heat is transported in the system. For relatively low modulation frequencies we notice only a small effect on the time-averaged  $Nu$ , while the response becomes considerably more dynamic with higher frequencies in the  $Nu$  signal as well as stronger fluctuations. If the modulation frequency is increased sufficiently, e.g.,  $Ro_\omega = 0.1$ ,  $0.2$ , we notice that the time-averaged  $Nu$  is considerably increased and that the dynamics of the  $Nu$  response is qualitatively altered. In fact, we observe rather long periods in which the Nusselt number is seen to increase to instantaneous values about two to three times as large as the constant rotation case, followed by quite dramatic collapse of  $Nu$  roughly to the level of the constant rotation case. The lengthy build-up phases at low  $Ro_\omega$  take several periods of the modulation procedure, i.e., these correspond to a



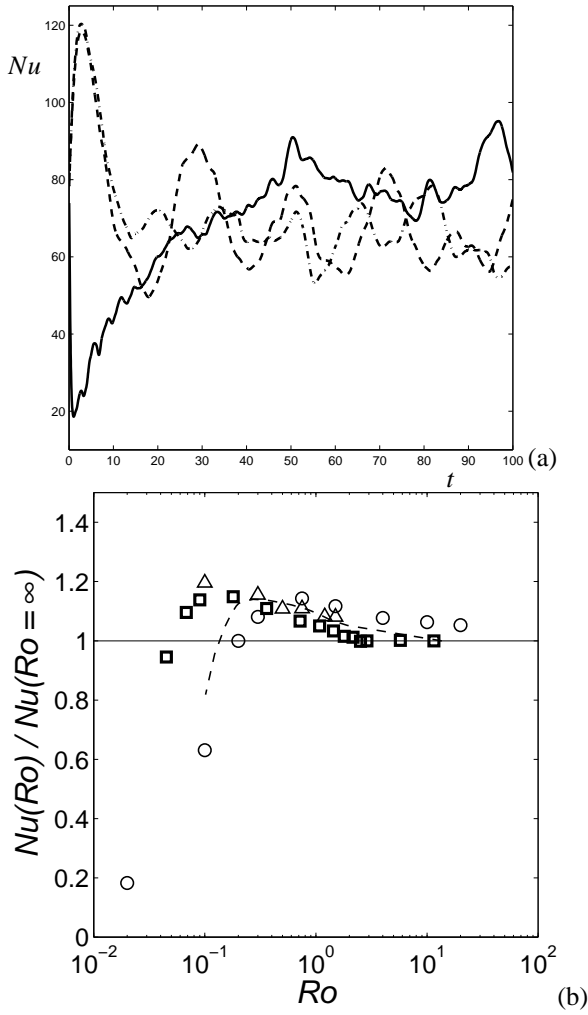


Figure 4. (a) Time-dependent  $Nu$  at constant rotation rate:  $Ro_0 = 0.1$  (solid),  $Ro_0 = 2.45$  (dash),  $Ro_0 = 5$  (dash-dot). (b) Time-averaged relative Nusselt number  $Nu(Ro_0)/Nu(Ro_0 = \infty)$  as a function of  $Ro_0$  with simulation results labeled with squares, comparing with findings from literature (Kunnen *et al.* (2008) and references therein).

long time-scale for the flow. During the build-up phases  $Nu$  oscillates considerably, at a frequency that corresponds approximately to twice the modulation frequency. The rather dramatic and rapid collapse of  $Nu$  as seen for  $Ro_\omega \leq 0.2$  is less frequent with decreasing modulation frequency. So, in case the Euler forces dominate the dynamics  $Nu$  oscillates rapidly during slow build-up phases, reaches high values, i.e., induces an effective flow structure for thermal transport and collapses vigorously to initiate the next build-up phase.

In order to appreciate the observed collapse of the Nusselt number in the strongly time-modulated rotation case, we illustrate a particular event in Figure 6 in case  $Ro_\omega = 0.2$ . The precise time history of the Nusselt number in Figure 6(a) shows a reduction in  $Nu$  of about 80 units from a high value around 135 to a low value of approximately 55, in about 7 dimensionless time units. This is quite fast compared to the general period of build-up of  $Nu$  which may be estimated around 35 time units at the selected parameters. The reason for this strong reduction in  $Nu$  may readily be seen in Figure 6(b, c). In fact, just before the  $Nu$ -collapse the temperature contours in the thermal column near the

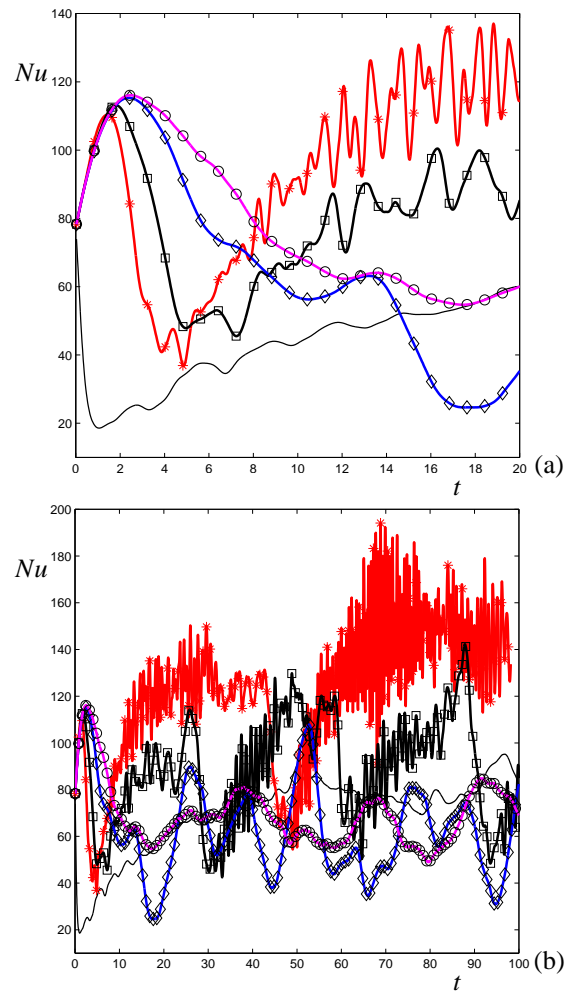


Figure 5. Time-dependent Nusselt number obtained for time-modulated rotation rates with  $Ro_0 = 2.45$ ,  $Ro^* = 2.55$  and varying modulation frequencies  $Ro_\omega$ : 0.1 (asterisks), 0.2 (squares), 0.5 (diamonds), 1 (circles). Also included is the constant rotation case at  $Ro_0 = 0.1$  (thin solid line). In (a) we show a detailed view for  $t \leq 20$  while (b) displays the long-time behavior, showing for  $Ro_\omega \leq 0.2$  clear build-up of  $Nu$  to rather high values, followed by abrupt collapse.

centerline show a considerable focussing of heat transfer by a large temperature gradient near the middle of the domain where red and blue isosurfaces almost intersect. Just after a  $Nu$ -collapse the gradually build up thermal column is seen to have almost completely disappeared and a much reduced temperature gradient remains.

## CONCLUDING REMARKS

In this paper we presented DNS results of time-modulated rotating Rayleigh-Bénard convection in a cylindrical domain of unit aspect ratio. The inclusion of a time-dependent rotation rate introduces an additional term in the equations which represents the so-called Euler force. This force acts in the circumferential direction only and may qualitatively alter the flow from a condition of a domain filling large-scale circulation (at low constant rotation rates) or dispersed local thermal plumes (at high constant rotation rates), to a more or less segregated situation in which a pronounced thermal column forms along the centerline of the

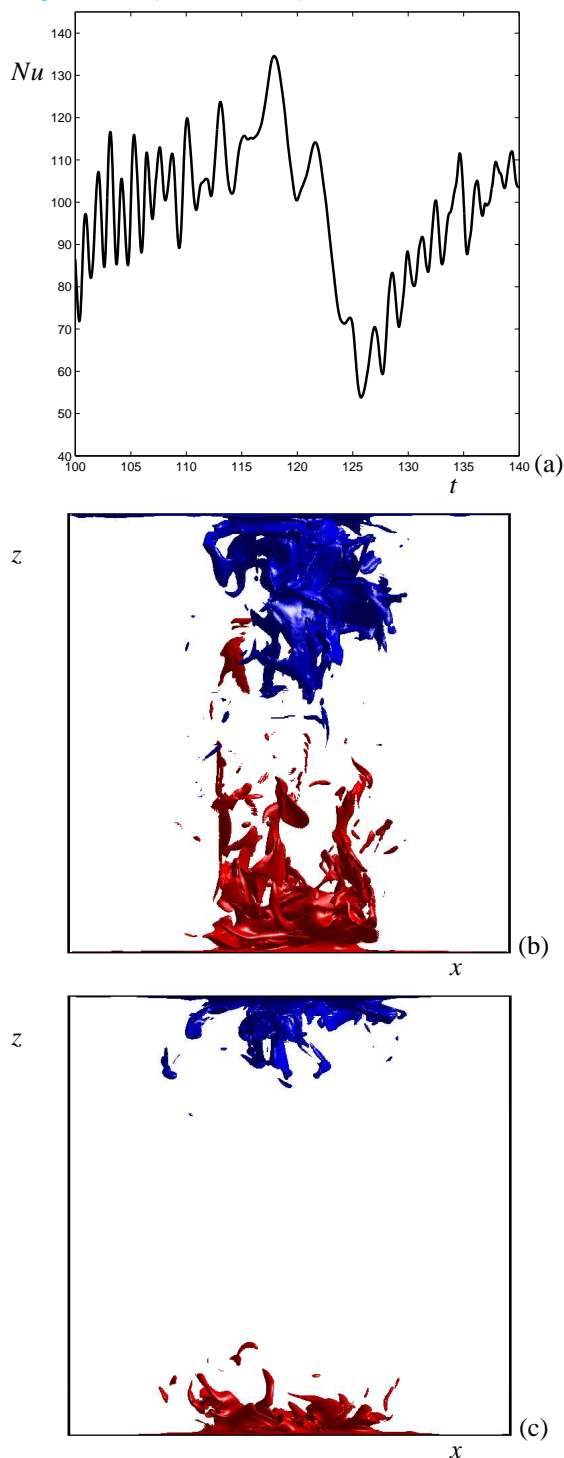


Figure 6. Illustration of a Nusselt collapse event occurring around  $t = 120$  for a time-modulated rotation rate at  $Ro_\omega = 0.2$ . In (a) the time-history of  $Nu$  is shown and in (b) and (c) the instantaneous solution for the temperature is depicted in a side view, just before ( $t = 117$ ) and just after ( $t = 125$ ) the collapse.

domain and highly sheared structures appear in the boundary layer near the vertical sidewalls.

A dominant Euler force was shown to yield very complex flow dynamics in which a long-time build-up of thermal structures arises in an oscillating manner, interspersed

by events of very abrupt and considerable collapse with associated strong reduction of the thermal transport efficiency, as quantified by the Nusselt number. This presents an interesting challenge in physical control of such turbulent flow, aimed at building up high- $Nu$  flow structures by modulated rotation. If such physical flow control could be developed such that the collapse events can be avoided, e.g., by properly changing  $Ro_\omega$  to maintain the main thermal column, then this phenomenon could find its way into technological applications that involve rotating heat transfer. This is subject of ongoing research.

## Acknowledgement

The computations were made possible by a grant from the Dutch National Science Foundation (NWO), executed at SARA (Grant SH-061).

## REFERENCES

- Ahlers, G., Grossmann, S. & Lohse, D. 2009 Heat transfer and large scale dynamics in turbulent Rayleigh-Bénard convection. *Rev. Mod. Phys.* **81**, 503–537.
- Geurts B.J. ed. 2001 *Modern simulation strategies for turbulent flow*. Edwards Publishing.
- Geurts B.J. 2003 *Elements of Direct and Large-Eddy Simulation*. Edwards Publishing.
- Julien, K., Legg, S., McWilliams, J. & Werne, J. 1996 Rapidly rotating turbulent Rayleigh-Bénard convection. *J. Fluid Mech.* **322**, 243–273.
- Kuczaj, A.K., Geurts, B.J. & Lohse, D. 2006 Response maxima in time-modulated turbulence: Direct numerical simulations. *EPL (Europhysics Letters)* **73** 851
- Kunnen R.P.J., Clercx H.J.H. & Geurts B.J. 2006 Heat flux intensification by vortical flow localization in rotating convection. *Phys. Rev. E* **74**, 056306.
- Kunnen R.P.J. Turbulent Rotating Convection *Thesis - Eindhoven University of Technology*
- Kunnen R.P.J., Clercx H.J.H. & Geurts B.J. 2008 Break-down of large-scale circulation in turbulent rotating convection *EPL (Europhysics Letters)* **84** 24001.
- Kunnen, R.P.J., Geurts, B.J. & Clercx, H.J.H. 2010 Experimental and numerical investigation of turbulent convection in a rotating cylinder. *J. Fluid Mech.* **642**, 445–476.
- Liu, Y., Ecke, R.E. 1997 Heat transport scaling in turbulent Rayleigh-Bénard convection: effects of rotation and Prandtl number. *Phys. Rev. Lett.* **79**, 22572260.
- Niemela J.J., Babuin S. & Sreenivasan K.R. 2010 Turbulent rotating convection at high Rayleigh and Taylor numbers *J. Fluid Mech.* **649**, 509–522.
- Oresta, P., Stringano, G., Verzicco, R. 2007 Transitional regimes and rotation effects in Rayleigh-Bénard convection in a slender cylindrical cell. *Eur. J. Mech. B/Fluids* **26**, 114.
- Rossby, H.T. 1969 A study of Bénard convection with and without rotation. *J. Fluid Mech.* **36**, 309335.
- Stevens, R.J.A.M., Clercx, H.J.H. & Lohse, D. 2010 Optimal Prandtl number for heat transfer in rotating Rayleigh-Bénard convection. *New J. Phys.* **12**, 075005.
- Verzicco R. & Orlandi P. 1996 A finite-difference scheme for three-dimensional incompressible flow in cylindrical coordinates *J. Comput. Phys.* **123**, 402413.